



HAL
open science

Beryllium bonding: insights from the σ -and π -holes analysis

M Esmail Alikhani

► **To cite this version:**

M Esmail Alikhani. Beryllium bonding: insights from the σ -and π -holes analysis. *Journal of Molecular Modeling*, 2020, 26 (5), pp.94. 10.1007/s00894-020-4348-1 . hal-02879141

HAL Id: hal-02879141

<https://hal.sorbonne-universite.fr/hal-02879141v1>

Submitted on 23 Jun 2020

HAL is a multi-disciplinary open access archive for the deposit and dissemination of scientific research documents, whether they are published or not. The documents may come from teaching and research institutions in France or abroad, or from public or private research centers.

L'archive ouverte pluridisciplinaire **HAL**, est destinée au dépôt et à la diffusion de documents scientifiques de niveau recherche, publiés ou non, émanant des établissements d'enseignement et de recherche français ou étrangers, des laboratoires publics ou privés.

Beryllium bonding: insights from the σ - and π -holes analysis[†]

M. Esmail Alikhani^{a,1}

^a*Sorbonne Université, CNRS, UMR 8233, MONARIS, Case courrier 49, 4 place Jussieu, F-75005, Paris, France*

Abstract

Beryllium bonding is actually a subclass of secondary bonding. Similar to the case of halogen bonding, the σ - and π -holes on the Be atom of the monomers give in zeroth-approximation the direction of electrophilic attack favorable to the formation of beryllium bonds. The nature of beryllium bonding is purely electrostatic so that the SAPT energy decomposition perfectly explains the relevance of the polarization- and dispersion-contribution on the formation of the beryllium bond.

Keywords: Beryllium bonding, MEP, σ - and π -holes, ELF and QTAIM topology, SAPT

1. Introduction

Beryllium is the smallest metal atom of the periodic table. It has been known since 1798 and was synthesized in its metallic form in 1828. [1] Its alloys are widely used in the space industry. The Be^{2+} cation is known as one of the hardest Lewis acids. However, research on beryllium chemistry is the least investigated and actually inhibited on the experimental side because of the extreme toxicity of Be metals, Be-containing salts and compounds. [2, 3] Although the number of compounds containing Be recorded in the Cambridge Structural Database is very limited compared to those of Mg and Al,[2] it should be emphasized that major advances have been made in the area of organometallic chemistry of Be in the recent two decades both from experimental and theoretical modeling perspective. [1, 2, 4]

Beryllium Bonds were first defined and characterized in 2009 by Yáñez, Mó and coworkers who considered the complexes between BeX_2 ($X = \text{H}, \text{F}, \text{Cl}, \text{OH}$) with different Lewis bases. [5] They underlined that although beryllium bonds are in general stronger than hydrogen bonds, they share many common features. Like the case of hydrogen bonds, [6, 7] cooperativity is also an important characteristic of beryllium bonds.[3] For instance, it has been shown that a weak noncovalent interaction, such as halogen- and hydrogen-bond, is reinforced through cooperativity with beryllium bonds. [8–10]

Unlike the beryllium bonds in which the Be atom is usually in its +2 formal oxidation state and forms very stable complexes with Lewis bases, [11, 12] Frenking and coworkers introduced a new class of beryllium containing compounds in which a neutral zero-valent $\text{Be}^{(0)}$ atom is stabilized by a strongly σ -donating and a good π -acidic cyclic (alkyl)(amino) carbene (cAAC).[13] Recently, Braunschweig and coworkers synthesized and characterized a dicoordinated $\text{Be}^{(0)}$ complex $[\text{Be}(\text{cAAC}^{\text{Me}})_2]$. [14]

Concerning the question of nomenclature, we note two great families of thought that each of them expresses and evokes precise information. First, researchers who prefer to continue with a nomenclature related to the chemical families of the periodic table, [15] second, researchers

[†]Dedicated to Nohad Gresh, a friend and a scientist, for his important contribution on secondary interactions.

¹E-mail: esmail.alikhani@sorbonne-universite.fr

who prefer to use a collective name that already coined by Alcock: "secondary bond". [16–18] I willingly belong to the second family of thought.

The reactivity of various simple aldehydes towards beryllium halides was published in 2019. [19] Beryllium chemistry has become an interesting topic for researchers. In order to go further in understanding the nature of beryllium binding, we propose in this paper a new look to the Be(II)-Ligand bonding obtained from energetic decomposition, molecular electrostatic properties, and electron localization function topology.

2. Computational details

The calculations were carried out with the Gaussian 09 program. [20] Geometrical optimization and vibrational frequency calculation were done at two levels of theory:

- the coupled cluster single-double and perturbative triple excitations CCSD(T) [21–27] with triple- ζ correlated consisting basis set of Dunning aug-cc-pVTZ [28]
- the popular three parameters functional B3LYP [29] including in addition the GD3BJ correction for dispersion contributions [30] with the Ahlrichs basis sets Def2-TZVPP [31, 32]

In this paper, unless explicitly stated, geometric optimization has been done at the B3LYP-GD3BJ/Def2-TZVPP computational level.

Energy decomposition from wavefunction-based Symmetry Adapted Perturbation Theory (SAPT) was carried out on the optimized geometry at SAPT2+3 level [33, 34] in conjunction with Aug-cc-pVDZ basis set using the Psi4 program. [35, 36]

Molecular electrostatic potential surfaces (MEP) mapped on the 0.001 *a.u.* electron density for the isolated monomers were calculated at the B3LYP-GD3BJ/Def2VTZPP computational level. MEP surfaces have been generated using the "wfx" files by AIMALL software.[37] Maxima and minima of the MEP on the isodensity surface were found using Multiwfn program. [38] Let me emphasize that in this article we express the MEP in energy units (*kcal/mol*) rather than units of potential (*volts*). When we give the MEP value at \mathbf{r} in energy, this means that the MEP corresponds to the interaction energy with a +1 point charge located at \mathbf{r} .

The topology of the electron density provide a unique definition of atoms in molecules: Quantum Theory of Atoms In Molecules (QTAIM). [39, 40] The interaction of two atoms at any separation results in the formation of critical point (CP) in the electron density, a point where its gradient $\nabla\rho(\mathbf{r})$ vanishes. A bond critical point (BCP) is a CP with the two negative curvatures. Two bonded atoms are characterized by the existence of a BCP. QTAIM calculations have been performed using the AIMALL program [37].

The electron localization function (ELF) [41] has been used to partitioning the molecular space in core and valence basins. The topological valence basin properties have been analysed within the ELF topology using the TopMod program. [42] The ELF function, as defined by Silvi and Savin, [43] obeys the following equality relation: $0 \leq \eta \leq 1.0$ and a value of the ELF – noted as η – close to one corresponds to a region of the space where there is a high probability of finding electron localization, whereas an ELF value close to 0.5 corresponds to a region of electron gas-like behaviour.

3. Results and discussion

In order to illustrate σ - and π -hole properties, interaction between one or two bases and Be(II) containing molecules – namely BeNH presenting a σ -hole on Be atom, and BeCl₂ with a π -hole – have been investigated in this paper.

3.1. σ - and π -holes on the monomers

To identify the electrophilic regions (σ - and π -holes), the MEP and ELF basins of both BeNH and BeCl₂ are illustrated in Figure 1, with BeNH in the first row and BeCl₂ in the second one.

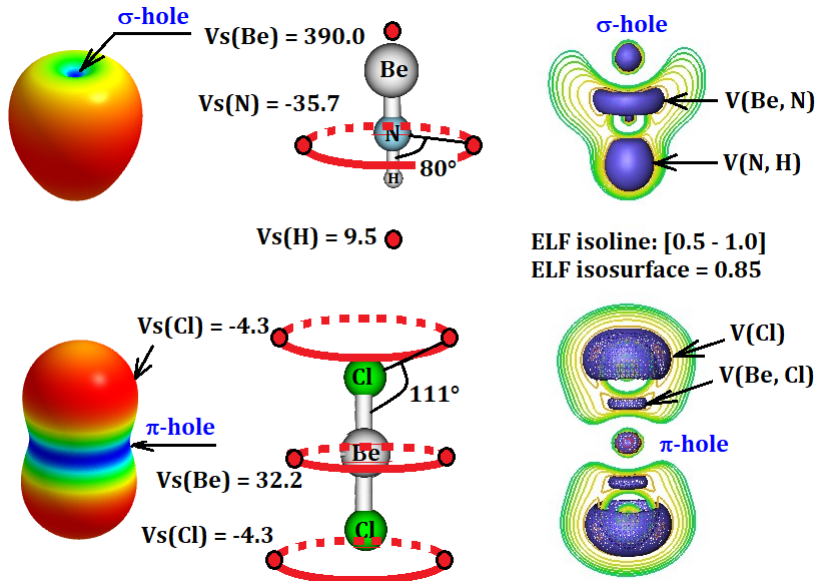


Figure 1: MESP isosurfaces on the 0.001 au electron density isosurface (left column), MEP critical points (second column), and ELF isolines (right column) for the isolated monomers, calculated at the B3LYP-GD3BJ/Def2-TZVPP computational level. At local maxima and minima, the electrostatic potential values are in kcal.mol⁻¹.

The MEPs on the 0.001 *a.u.* electron density isosurface are displayed in the left column where red and blue regions indicate negative and positive potentials, respectively. The potential value (in kcal.mol⁻¹) at the critical points of the MEP isosurface are reported in the central column in Figure 1. The electrostatic potential (ESP) value at the σ -hole of BeNH is particularly high, 390.0 kcal.mol⁻¹ while the ESP maximum on the BeCl₂ is only 32.2 kcal.mol⁻¹ and forms a belt around the beryllium atom (π -hole). However, we should note that we found a region of positive electrostatic potential (1.2 kcal.mol⁻¹) located on the chlorine atom on the extension of Be–Cl bond which naturally corresponds to the Cl σ -hole (Fig. 2).

We note also two other distinct regions on the MEP of BeNH molecule which correspond to the lone-pair of nitrogen ($V_s(\text{N}) = -35.7$ kcal.mol⁻¹) and to the σ -hole on the H atom ($V_s(\text{H}) = 9.5$ kcal.mol⁻¹). The critical point at the N lone-pair forms an angle equal to 80° with N–H bond. In BeCl₂, the Cl lone-pair ($V_s(\text{Cl}) = -4.3$ kcal.mol⁻¹) forms an angle of 111° with Be–Cl bond.

The ELF basins are depicted in the right column, for the $\eta = 0.85$ isosurfaces and $\eta \in [0.5 - 1.0]$ isolines. The BeNH and BeCl₂ are characterized by two and four irreducible localization domains, respectively. We remember that a *f*-localization domain is an isosurface with the restriction that each point satisfies $ELF(\mathbf{r}) > f$. Two irreducible localization domains within BeNH, $V(\text{Be}, \text{N})$ and $V(\text{N}, \text{H})$, correspond to the Be–N and N–H bonds. Nevertheless, a closer look to the isolines surrounding the N and H atoms for $ELF = 0.5$ clearly indicates that $V(\text{Be}, \text{N})$ valence basin with a population of 5.68 e^- is actually the ELF basin of the N lone-pair. Furthermore, the ELF population of the NH electron withdrawing fragment was calculated to be $\bar{N}(\text{NH}) = 9.93e^-$ with a variance $\sigma^2 = 0.17$. These considerations illustrate that the formal oxidation state of Be is +2 within free BeNH molecule. The shape of the ELF localization domain of the NH fragment obviously shows electrophilic region away from Be–N bond. For the case of BeCl₂, a toroidal region around the beryllium atom where even the $\eta = 0.5$ isolines are absent illustrates an electrophilic region from the ELF analysis.

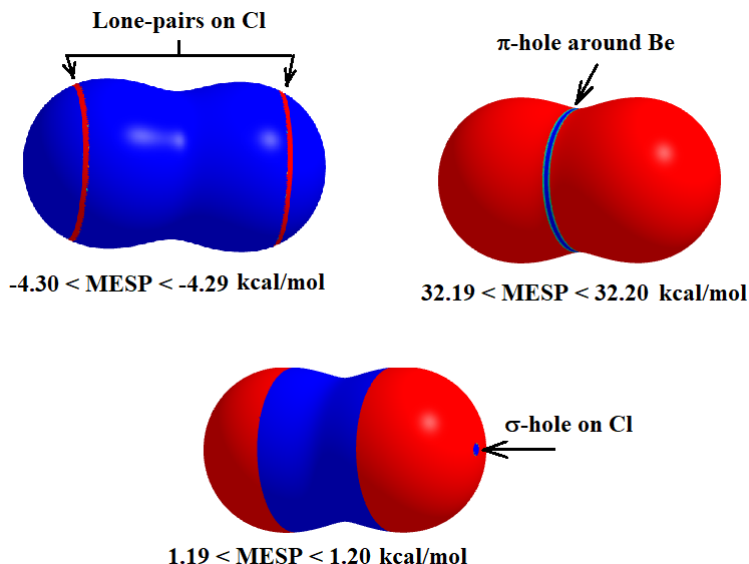


Figure 2: MESP isosurfaces over very close range on the 0.001 au electron density isosurface of free BeCl₂, calculated at the B3LYP-GD3BJ/Def2-TZVPP computational level.

Evidently, the MEP topography and the ELF topology provide complementary information to characterize the molecular electrophilic sites. [44]

3.2. Strong Beryllium σ -hole: attractive interaction between noble gases and BeNH

Thanks to their completely filled valence electronic configuration, the noble gases (Ngs) are the least reactive elements in the periodic table compared to the other elements. As a result, Ngs atoms hardly react as Lewis acids or Lewis bases. Energetically favourable intermolecular interactions between the covalently bonded Ngs atoms and the Lewis base centres were reported in the literature. Ng–XY interaction is known as "aerogen bonds", when the noble gas centre behaves as a Lewis acid in interaction with a Lewis base. [45–47]

Here, our study focuses on interactions between an Ng atom and σ -hole of BeNH. Optimization and vibrational frequency calculations have been done at the CCSD(T)/Aug-cc-pVTZ level of theory. Five interactions studied here belong to the $C_{\infty v}$ group. In Table 1 are gathered energetic, geometrical properties as well as harmonic vibrational frequencies. For the lighter noble gases complexed with BeNH, our theoretical results are very close to those published previously at the CCSD(T) level also but with a smaller basis set, 6-311G(d,p). [48]

Complex	r(Be-N)	r(Be-Ng)	D_0	$\Delta(\Delta G)$	ν_2	ν_3
Free BeNH	1.364				1557	
He–BeNH	1.366	1.494	-5.2	-6.7	1571	552
Ne–BeNH	1.365	1.798	-4.6	-7.5	1569	259
Ar–BeNH	1.369	2.069	-11.6	-15.0	1561	285
Kr–BeNH	1.371	2.190	-15.2	-19.2	1555	265
Xe–BeNH	1.373	2.357	-18.4	-22.9	1545	253

Table 1: CCSD(T) binding energy (D_0), free-energy change ($\Delta(\Delta G)$) in kcal.mol⁻¹, optimized bond length (Å), and harmonic vibrational frequencies (cm⁻¹) of the singlet ground state Ng–BeNH.

Compared to the Be–N bond length in free BeNH, this distance slightly increases to a thousandth of angstrom upon complexation. The Be–Ng interatomic distance increases with the Ngs atomic radii. Binding energy corrected for the zero-point energy (referred to as D_0) decreases in going from He–BeNH to Ne–BeNH, and then steadily increases up to Xe–BeNH.

However, as expected, the greater the polarizability of Ng, the higher the energetic stability of Ng–BeNH. It is interesting to note that all the five molecules are exergonic with $\Delta(\Delta G) < 0$.

Surprisingly, the ν_2 normal mode frequency variation does not follow that of Be–N bond length. We assigned this normal mode using potential energy distribution (PED) analysis of all the fundamental vibration modes by the use of the VEDA 4 program. [49, 50] The Q_2 normal coordinate (corresponding to the ν_2 normal mode) was defined by a linear combination between three internal coordinates, namely $s_1 = Be - H$, $s_2 = Be - N$, and $s_3 = Be - Ng$. The PED analysis has clearly shown that the ν_2 normal mode corresponds exclusively to the ν_{Be-N} stretching mode in the case of BeNH molecule, while the ν_{Be-N} and ν_{Be-Ng} stretching modes are coupled in ν_2 for Ng–BeNH. In the latter case, the contribution of ν_{Be-N} stretching mode is close to 95%. In other words, the apparent inconsistency between the Be–N bond length variation and the ν_2 frequency evolution upon complexation with different Ng atoms can be explained by the fact that the ν_2 frequency reported in Table 1 does not correspond only to the ν_{Be-N} stretching mode, but rather to a linear combination of two stretching modes.

On the ground of qualitative arguments supported by the topology of Atoms In Molecules theory, [52] Frenking and co-workers [51] and later Borocci and co-workers [53] clearly pointed out that the Be–He interaction in both He–BeO and H₃BOBe–He is essentially electrostatic, since the charge transfer from helium to beryllium is practically negligible, if any, and the Laplacian of the electron density at the Be–He bond critical point is large and positive. Are these features common to the case of Ng–BeNH complex? In order to answer this question, we will present below our results obtained by two approaches: i) qualitative analysis of the ELF valence basins, and ii) quantitative analysis of energy decomposition in the frame of the SAPT theory.

ELF contour line and isosurface diagrams are illustrated in Figure 3. This figure is composed of two columns and three rows. In the first row are depicted He–BeNH and Ne–BeNH. In the second row are displayed Ar–BeNH and Kr–BeNH. The ELF contour line (2D) and isosurface (3D) diagram of Xe–BeNH are presented in the third row. A careful look at the ELF diagram reveals that the localization domain of Ng is no longer spherical, but indicates a net deformation in front of the Be atom. Inspection of the contour lines in Figure 3, however, suggests that the valence electron localization domain of the Ng atom is polarized toward the Be atom. Furthermore, a closer look at the valence contour lines (2D) reveals an increasing polarization of the valence basin of the Ng atom toward BeNH when going from He to Xe. Interestingly, the ELF valence basin is a single irreducible localization domain in the case of lighter noble gases (*i.e.* He-, Ne-, and Ar–BeNH), but it appears three new irreducible localization domains with $\eta = 0.80$ in the case of Kr-, and Xe–BeNH. These domains are indicated by a red "+" symbol and labelled as LP1(Ng), LP2(Ng), and LP3(Ng) for $\eta = 0.80$ in Figure 3. As illustrated by the figure reported in the last column and last row, the first region located between Ng and Be actually reflects a disynaptic valence basin of the noble gas atom shared by two Ng and Be nuclei, whereas two external 2D regions – labelled as LP2(Ng) and LP3(Ng) – correspond to a toroidal valence basin of the Noble gas (*i.e.* V(Kr) and V(Xe)). The average population of the shared valence basin is slightly greater than $2 e^-$, $2.11 e^-$ and $2.16 e^-$ for Kr and Xe, respectively. However, it should be pointed out that appearance of the LP1(Ng) valence basin, although shared, is a consequence of the strong polarization of the valence sphere of Kr and Xe induced by the electric field of HNBe characterized by the σ -hole of Be. Accordingly, the ELF features mirror the coulombic interaction between the strong σ -hole on the beryllium atom and the electronic cloud of noble gas atom.

It is evident from above discussion that the polarization of each partner upon interaction must be taken into account to properly describe the coulombic interaction between a noble gas atom and the beryllium σ -hole. Consequently, in order to provide a quantified analysis we used "SAPT2+3" level which includes many-body treatment of the intramolecular correlation po-

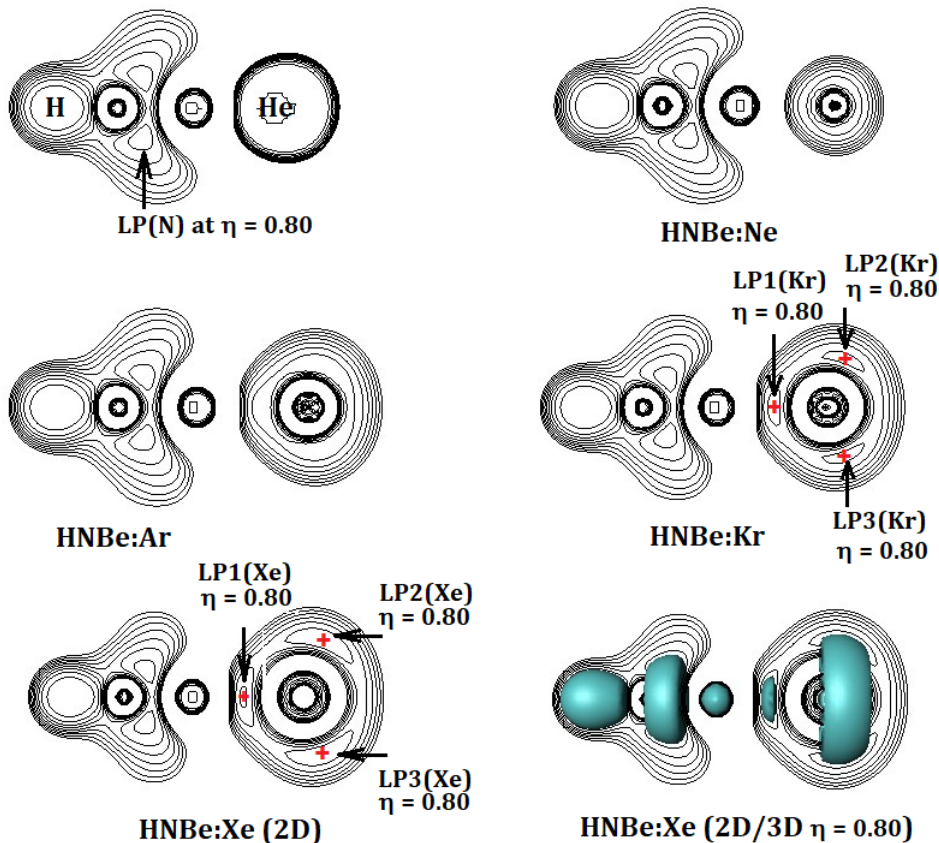


Figure 3: ELF $\eta \in [0.5 - 1.0]$ isolines and $\eta = 0.80$ isosurface of Ng–BeNH($^1\Sigma$). The most external isoline corresponds to $\eta = 0.50$

tentials and higher-order terms. [33] One powerful feature of SAPT is that it provides a decomposition of the inter-molecular interaction energy in terms of physically intuitive electrostatic, exchange, induction, and dispersion components. Partitioning of the inter-monomer interaction energy (E_{int}) at the CCSD(T) optimized geometry includes short-range exchange–repulsion (E_{ee}), electrostatics (E_{ele} , *e.g.* charge–charge, charge–dipole, dipole–dipole, etc.), induction polarization (E_{ind} , *e.g.* dipole/induced-dipole) and London dispersion forces (E_{disp} , *e.g.* instantaneous dipole/induced dipole). We must always have in mind that the $E_{elst} = E_{ele} + E_{ee}$ term representing the electrostatic interaction between the unperturbed molecules only corresponds to a part of the total electrostatic (or coulombic) interaction. Mutual polarization and dispersion are two inherent components of total electrostatic energy. [54, 55] It should be noted that the deformation energy, which reflects the change in energy originating from the deformation of the monomers upon the formation of the complex, was not included in the inter-monomer interaction energy. It is therefore expected that the SAPT E_{int} is slightly different from the binding energy (D_e) since the latter is calculated with respect to free subunits in their optimized geometries. In Table 2 are reported SAPT2+3/Aug-cc-pVDZ decomposition of the interaction energy (in kcal.mol $^{-1}$) at the CCSD(T)/Aug-cc-pVTZ optimized geometry. The different energetic contributions satisfy the following relation:

$$E_{int} = E_{elst} + E_{ind} + E_{disp}$$

As expected, the SAPT2+3 decomposition shows that electrostatics contribution between a noble gas atom and a polar molecule is actually negligible, whereas the exchange repulsion is high compared to the interaction energy ($E_{int}(sapt2+3)$). We note also the polarization contribution is nearly four times larger than the dispersion one, and in absolute value two times larger than the exchange-repulsion term. Accordingly, in all the Ng–BeNH complexes,

Contribution	He–BeNH	Ne–BeNH	Ar–BeNH	Kr–BeNH	OC–BeNH
E_{ele}	0.35	-0.04	-0.03	-0.04	-24.8
E_{ee}	4.19	5.63	11.12	12.64	30.1
$E_{elst} = E_{ele} + E_{ee}$	4.54	5.59	11.09	12.60	5.3
E_{ind}	-7.91	-8.26	-17.0	-20.11	-34.7
E_{disp}	-1.69	-1.87	-4.41	-5.33	-8.4
$E_{int}(\text{sapt2+3})$	-5.06	-4.54	-10.32	-12.84	-37.8

Table 2: SAPT2+3 energetic contributions (kcal.mol⁻¹) at CCSD(T) minimum for various studied complexes.

the dominant term is by far the induction (polarization) energy, while dispersion plays a minor role.

To further the discussion, we optimized the complex formed between CO and BeNH when the Be σ -hole interacts favorably with the carbon lone-pair of CO. The binding energy of such an interaction was found to be -43.1 kcal.mol⁻¹, calculated at the computational CCSD (T) / Aug-cc-pVTZ level. The SAPT decomposition, reported in the last column of Table 2, shows that the electrostatic contribution alone almost cancels the exchange-repulsion term. Here again, the polarization contribution is nearly four times larger than the dispersion. Unlike the Ng–BeNH, only the dispersion contribution is sufficient to overcome the repulsion due to $E_{elst} = E_{ele} + E_{ee}$ and stabilize the complex. It is therefore evident that the mutual polarization of each partner is intrinsic to the Ng–Be interaction.

3.3. Beryllium π -hole: mono- and di-ligated complexes with BeCl_2

Nowadays, density functional theory is widely used to study the different properties of chemical compounds. Here, we use the popular three parameters B3LYP functional to optimize and calculate the harmonic vibrational frequencies for several chemical systems containing the BeCl_2 group. Calculations were carried out with the B3LYP functional corrected for dispersion contribution using the empiric Grimme GD3 dispersion with Becke-Johnson damping (referred to as "B3LYP-GD3BJ"). [30]

In order to test the reliability of this DFT method for calculating geometrical and energetic properties, two complexes, Kr– BeCl_2 and OC– BeCl_2 were investigated at the CCSD(T)/Aug-cc-pVTZ level which is considered as an approach with a high accuracy. Optimized geometry parameters as well as the binding energy are reported in Figure 4 for both Kr– BeCl_2 and OC– BeCl_2 .

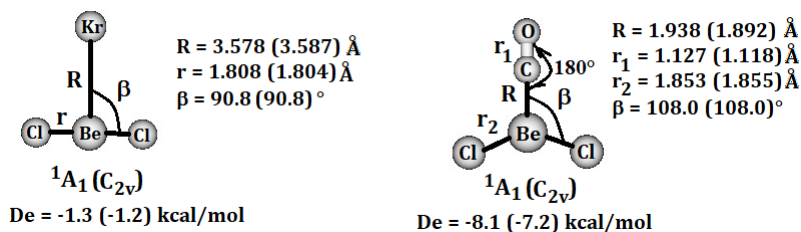


Figure 4: CCSD(T) and B3LYP-GD3BJ (reported in parentheses) as well as the binding energy for both Kr– BeCl_2 and OC– BeCl_2 in the 1A_1 electronic ground state.

For two rather weak noncovalent complexes, the agreement between geometrical parameters at the equilibrium geometry predicted by both methods is very nice. The Kr– BeCl_2 binding energy is predicted to be much smaller than the OC– BeCl_2 one. However, B3LYP-GD3BJ gives a binding energy very close to that calculated with CCSD(T).

In Table 3 are reported some relevant harmonic vibrational frequencies calculated with both CCSD(T)/aug-cc-pVTZ and B3LYP-GD3BJ/Def2-TZVPP methods.

Compound	Method	ν_{C-O}	ν_{BeCl}^{sym}	ν_{BeCl}^{asym}
Free CO	CCSD(T)	2144		
	B3LYP-GD3BJ	2214 (77)		
Free BeCl ₂	CCSD(T)		400	1138
	B3LYP-GD3BJ		395 (0)	1127 (449)
OC-BeCl ₂	CCSD(T)	2228	546	984
	B3LYP-GD3BJ	2278 (161)	549 (90)	963 (332)
Kr-BeCl ₂	CCSD(T)			1136
	B3LYP-GD3BJ			1125 (422)

Table 3: Some relevant vibrational frequencies (in cm^{-1}) calculated at both CCSD(T)/aug-cc-pVTZ and B3LYP-GD3BJ/Def2-TZVPP levels. In parentheses are given the absolute infrared intensities in km/mole .

The B3LYP-GD3BJ harmonic vibrational frequency shifts, calculated with respect to free monomers, are also very close to those obtained with CCSD(T) method. For Kr-BeCl₂, three most intense modes, C-O stretch and Be-Cl symmetric and asymmetric stretching, shifted by -64, +164, and -154 cm^{-1} at the B3LYP-GD3BJ computational level are in good agreement with the CCSD(T) results, -84, +154, and -146 cm^{-1} . The Be-Cl asymmetric stretching frequency shift is found to be very small (+2 cm^{-1}), as expected for the very weak Kr-BeCl₂ complex.

We can therefore conclude that the B3LYP functional corrected for the dispersion contribution, B3LYP-GD3BJ, in combination with a basis set of triple- ζ quality, Def2-TZVPP, is fully adequate to study the BeCl₂ containing molecular complexes.

As shown in Figures 1 and 2, the maximum obtained on the MEP surface of BeCl₂ surrounding as a belt the beryllium atom with an ESP value of 32.2 kcal.mol^{-1} illustrates the π -hole on the BeCl₂ molecule. This electrophilic region can interact favorably with negative regions on another molecule, such as Cl₂, NH₃, and DMF (dimethylformamide). Minimum values of the ESP found at the B3LYP-GD3BJ/Def2-TZVPP optimized geometry are -3.5, -38.7, and -43.4 kcal.mol^{-1} for Cl₂, NH₃, and DMF, respectively. It is interesting to note that the position of these minima determine the angular attack with respect to the π -hole. In the case of NH₃, the minimum on the MEP is on the C_3 axis passing through N atom. In the case of Cl₂, the critical point (CP) corresponding to the minimum on the MEP is found to be the Cl-Cl off-axis with an angle around $CP - \widehat{Cl} - Cl = 96^\circ$. For DMF, the critical point corresponding to the minimum on the MEP is localized on the carbonyl oxygen with an O-C off-axis angle of $CP - \widehat{O} - C = 156^\circ$.

As shown in Figure 5, the optimized geometry of H₃N-BeCl₂ fully agrees with the predicted angular attack: Be-N coincides with the local NH₃ C_3 and BeCl₂ C_2 axes, while we note a small deviation for two other complexes. The angle $Cl - \widehat{Cl} - Be$ in the Cl₂-BeCl₂ equilibrium geometry is larger than the predicted $CP - \widehat{Cl} - Cl$ by +20°. This deviation could be attributed to the repulsion between two electron rich regions on the free Cl atom of Cl₂ and a BeCl₂ Chlorine ($r(\text{Cl} \cdots \text{Cl}) = 3.819 \text{ \AA}$). The angular deviation is the largest in the case of DMF-BeCl₂ which rises to -32°. The decrease of the $Be - \widehat{O} - C$ angle with respect to $CP - \widehat{O} - C$ one is in fact due to the presence of an H-bond between Cl of BeCl₂ and H of DMF ($r(\text{H} \cdots \text{Cl}) = 2.634 \text{ \AA}$).

The binding energy calculated with respect to free BeCl₂, Cl₂, NH₃, and DMF are -5.1, -31.8, and -33.9 kcal.mol^{-1} for Cl₂-BeCl₂, NH₃-BeCl₂, and DMF-BeCl₂ complexes, respectively.

The SAPT decomposition (Table 4) clearly shows that the E_{elst} contribution corresponding to the electrostatic interaction between the electronically unperturbed monomers is too high in the case of Cl₂-BeCl₂ which contains a non-polar molecule, while it is nearly negligible for the other two complexes. However, the total interaction energy (labelled as $E_{int}(\text{sapt2+3})$ in

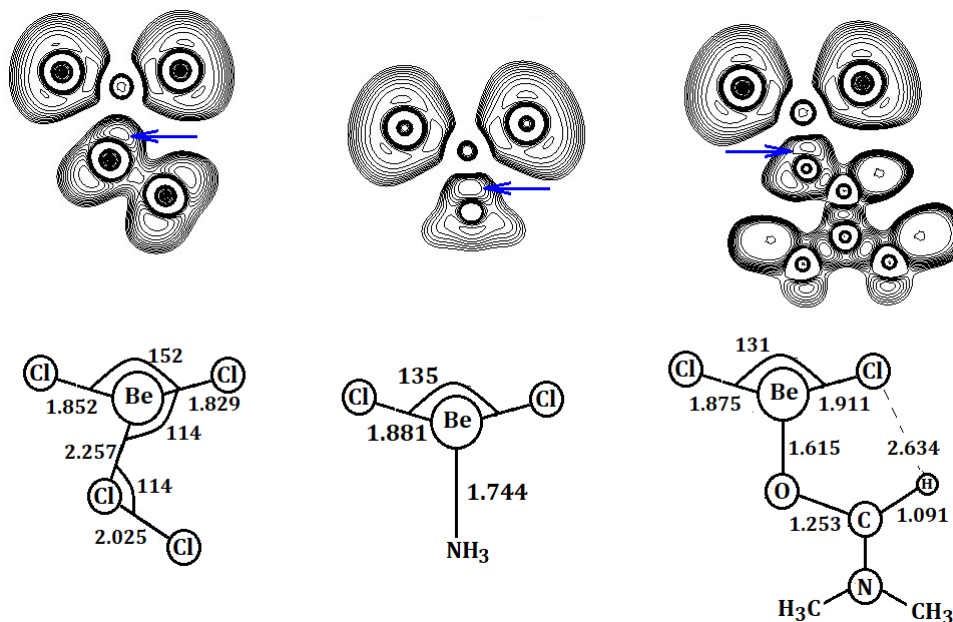


Figure 5: In first row are given the ELF isoline curves of three monoligated BeCl_2 complexes for $\eta \in [0.4 - 1.0]$. The electron rich valence basins (nucleophilic region) of ligand interacting with the π -hole of BeCl_2 are indicated by a blue arrow. The most relevant geometrical parameters (distance in Å and angles in degree) are depicted in second line.

Contribution	$\text{Cl}_2\text{-BeCl}_2$	$\text{NH}_3\text{-BeCl}_2$	DMF-BeCl_2
E_{ele}	-18.9	-70.1	-70.0
E_{ee}	38.8	71.7	73.2
$E_{elst} = E_{ele} + E_{ee}$	19.9	1.6	3.2
E_{ind}	-18.2	-37.0	-37.0
E_{disp}	-9.6	-10.8	-10.8
$E_{int}(\text{sapt2+3})$	-7.9	-46.3	-46.3
D_e	-5.1	-31.8	-38.7

Table 4: SAPT2+3 energetic contributions (kcal.mol^{-1}) at the equilibrium geometries.

Table 4) is enough stabilizing thanks to the $E_{ind} + E_{disp}$ contributions. Like the complexes studied in the §3.2, we note that the dispersion contribution does not exceed the half of the polarization one. We also notice that the binding energy is always higher than the SAPT interaction energies. This difference is essentially due to the deformation energy of the partners taken in their geometries of the equilibrium complex, and also to the use of different level of theory.

The most relevant geometrical change upon the formation of the complex concerns the BeCl_2 molecule: it bends away from the second molecule ($\widehat{\text{ClBeCl}} = 152^\circ$, 13° , and 131°), so that the bending angle lowers as the binding energy increases. As for the ligand, we note an increase in Cl-Cl and C=O bond distances of 0.01 and 0.04 Å compared to free ligands.

Beryllium dichloride is soluble in many N-donor and O-donor solvents. This leads usually to the pseudo-tetrahedral coordinated di-ligated adducts. [1, 12, 19, 56] Just to illustrate this point, we present di-ligated $(\text{DMF})_2\text{-BeCl}_2$ in Figure 6.

In Figure 6, we specially highlighted two groups of BCPs. The first one, labelled as BCP1, corresponds to the O-Be bond, while the second one (labelled as BCP2) stands for the $\text{H}\cdots\text{Cl}$ hydrogen-bond. The Laplacian of the electron density was found to be positive at both BCP1 and BCP2, indicating the presence of a closed-shell interaction between related atoms. The electron density which is usually used as a measure of the bond-strength [44, 57-59] is found

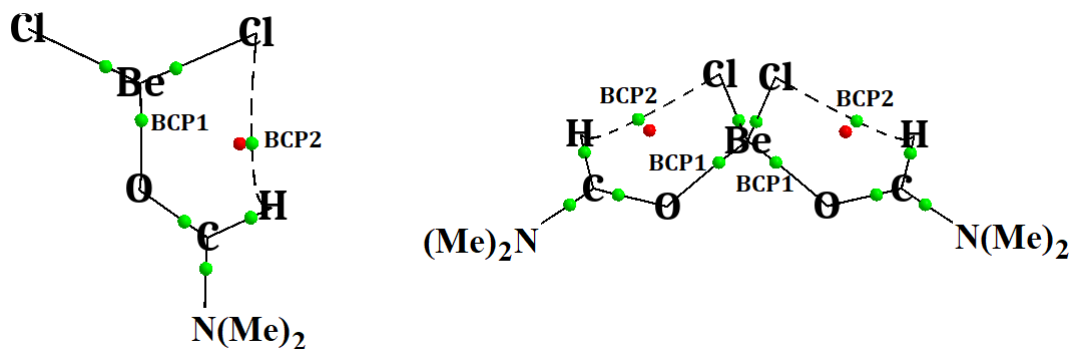


Figure 6: Pseudo-tetrahedral di-ligated $(\text{DMF})_2\text{-BeCl}_2$ compared to the mono-ligated DMF-BeCl_2 adduct. Small balls represent the bond critical point (green) and the ring critical point (red).

to be 0.014 a.u. at the BCP2 for both mono- and di-ligated adducts. In both adducts, the electron density at the BCP1(O–Be) is at least four times larger than that of BCP2. At our computational level, the electron density at BCP1 was found to be 0.074 a.u. for mono-ligated adduct, and 0.062 a.u. for di-ligated one. These topological changes are coherent with the change of the binding energy. The binding energy per ligand changes as follows: $-33.9 \text{ kcal.mol}^{-1}$ for DMF-BeCl_2 and $-27.3 \text{ kcal.mol}^{-1}$ for $(\text{DMF})_2\text{-BeCl}_2$. Finally, it is interesting to note that beryllium dichloride bends even more throughout the addition of a second ligand (*i.e.* from 131 to 118°).

3.4. Cooperativity induced by polarization

Cooperativity has been considered as the characteristic feature of secondary interactions in the literature. [6, 8–10, 60–67] That is, the intermolecular distance decreases as the intermolecular binding energy increases when the number of molecules involved in the complex increases.

Recently, Yáñez and co-workers investigated from theoretical point of view the cooperativity effect in several compounds containing the beryllium bonds. [8–10, 60, 61] They showed that the mutual influence between beryllium bonds and intermolecular halogen-bond [10] (or hydrogen-bond [8]) enables us to modulate the strength of halogen (or hydrogen) bonds. They explained this properties in terms of the changes in the atomic energy components calculated within the QTAIM framework and also in terms of the charge transfer using the natural bond orbital (NBO) method.

In order to explore the cooperative effects withing the molecular electrostatic topography, we present in this paragraph the case of a complex involving imidazole ($\text{C}_3\text{H}_4\text{N}_2$ noted as Im in the following), cyanogen chloride (ClCN), and beryllium imide (BeNH).

Some most relevant geometrical as well as energetic properties are displayed in Figure 7.

When we scrutinize the binding energy, we note that the relative binding energies of the ternary complex with respect to both binary adducts (-9.9 and $-58.5 \text{ kcal.mol}^{-1}$) are more negative than the binding energy of the binary complexes (-6.2 and $-54.8 \text{ kcal.mol}^{-1}$) for Im–ClCN and ClCN–BeNH, respectively). That is, the energetic stability of the halogen bond Im–ClCN and the beryllium bond ClCN–BeNH increase when the ClCN interacts simultaneously with Im and BeNH.

The MEP topography provides a simple and straightforward explanation for the bond-strengthening in ternary adduct.

As shown in Figure 8, the halogen-bond in the Im–ClCN binary complex is due to the interaction between the ESP minimum at Im and the ESP maximum at ClCN, *i.e.* -43 and $+37 \text{ kcal.mol}^{-1}$, while the same halogen-bond in the Im–(ClCN–BeNH) ternary complex is due to the interaction between the ESP minimum at Im and the ESP maximum at ClCN–BeNH,

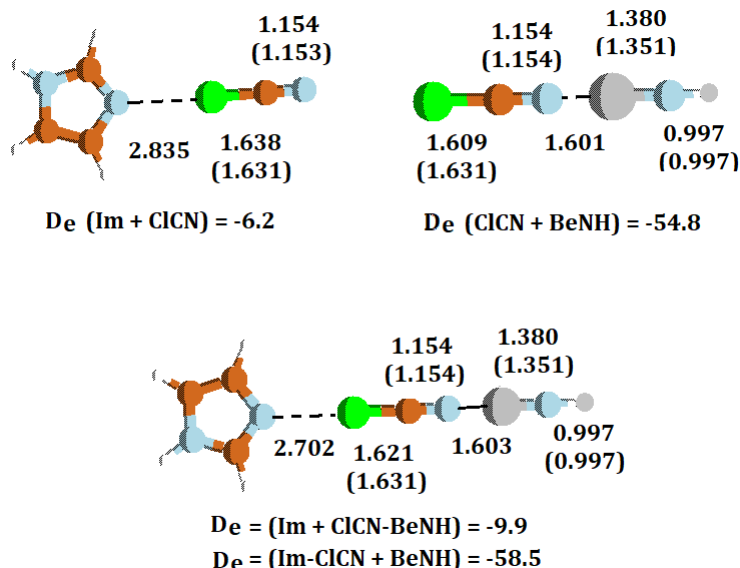


Figure 7: B3LYP-GD3BJ/Def2-TZVPP optimized geometries of two binary adducts, Im-ClCN and ClCN-BeNH, and one ternary complex, Im-ClCN-BeNH. Binding energies (labelled as D_e) are in kcal.mol⁻¹, and bond distances in Å. Note that values reported in parentheses are the bond lengths for free molecules.

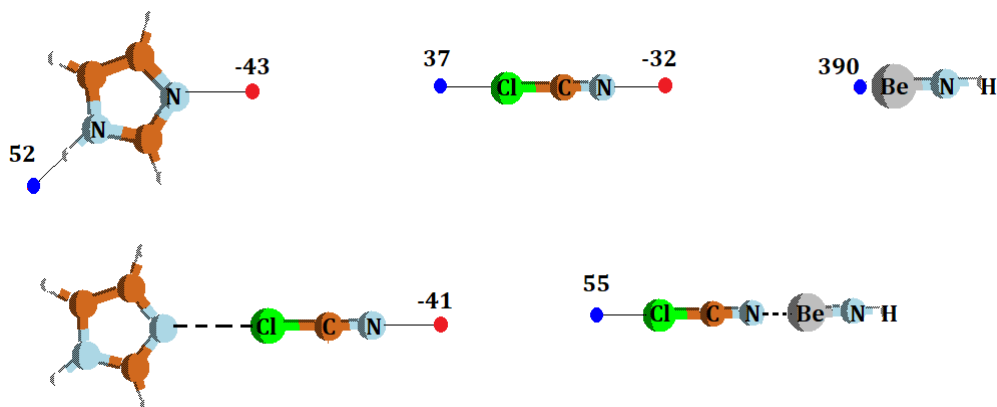


Figure 8: Some relevant critical points on the MEP surface for different subunits involved in the ternary Im-ClCN-BeNH complex. Blue and red dots indicates the location of the ESP maxima and minima.

i.e. -43 and +55 kcal.mol⁻¹. That means that the adding ClCN to BeNH leads to the formation of the beryllium bond and the strengthening of the σ -hole on the terminal Cl atom, 55 *vs.* +37 kcal.mol⁻¹. Consequently, the halogen bond between Im and ClCN-BeNH is stronger than that between Im and ClCN.

Similarly, we expect the interaction between Im-ClCN and BeNH to be stronger than that between ClCN and BeNH. That is, the σ -hole of BeNH (+390 kcal.mol⁻¹) interacts more favorably with the EPS minimum of Im-ClCN (-41 kcal.mol⁻¹) than with that of ClCN (-32 kcal.mol⁻¹).

Accordingly, a simplified means of understanding the cooperativity when we transform a binary adduct to a ternary one relies on consideration of how the formation of the dimer affects the minima and maxima EPS values.

The SAPT decomposition provides some insight into the participation of three energy components in the cooperativity, and indeed complements the aforementioned electrostatic analysis.

In Table 5 are reported SAPT2+3/Aug-cc-pVDZ decomposition of the interaction energy (in kcal.mol⁻¹) at the B3LYP-GD3BJ/Def2-TZVPP optimized geometries. For the Im-ClCN-BeNH ternary complex, the SAPT decomposition has been carried out in two ways: it has been

Contribution	ClCN–BeNH	(Im–ClCN)–BeNH	Im–ClCN	Im–(ClCN–BeNH)
E_{ele}	-39.2	-44.4	-9.1	-15.6
E_{ee}	35.1	35.6	9.8	14.7
$E_{elst} = E_{ele} + E_{ee}$	-4.1	-8.8	0.7	-0.9
E_{ind}	-35.4	-36.0	-2.8	-5.3
E_{disp}	-8.2	-8.3	-3.4	-4.2
$E_{int}(sapt2+3)$	-47.7	-53.1	-5.5	-10.4

Table 5: SAPT2+3 energetic contributions (kcal.mol⁻¹) at the B3LYP-GD3BJ/Def2-TZVPP optimized geometries.

considered as a binary complex once composed of (Im–ClCN) and BeNH, and a second time of Im and (ClCN–BeNH). Thus, we have been able to compare the ternary complex with both ClCN–BeNH and Im–ClCN binary complexes. A closer look at the different SAPT2+3 components reveals that the electrostatic change on the unperturbed interacting subunits alone explains the strengthening of the Be–N bond when we go from ClCN–BeNH to (Im–ClCN)–BeNH. While the simultaneous variation of the three components (E_{elst} , E_{ind} , and E_{disp}) contributes to the strengthening of the bond Im–Cl when we compare Im–ClCN to Im–(ClCN–BeNH). Note however that it is the polarization that changes much more than the other two components.

4. Conclusion

The term "Beryllium-bond" was proposed ten years ago by Yáñez and co-workers to design the interaction between the Be atom of BeX₂ (X = H, F, Cl, OH) and the nucleophilic region of a base. Our work showed that the electrostatic model (including polarization and dispersion) is central to describing the nature of interaction and the bonding motifs involved in the beryllium bonds. Simple MEP based concepts, such as maxima (σ - and π -holes) and minima (nucleophilic regions), enable us to predict the preferred direction leading to the formation of secondary interaction. The formation of a beryllium bond in turn produces considerable changes due to the polarization effect in the MEP properties of the new compound. That is, some critical points disappear, and others become stronger (or weaker) leading to a new MEP diagram. The sequential tracking of the critical points observed on the MEP surface allows us to explain very simply the bond strengthening due to cooperativity. However, the SAPT decomposition provides a clear explanation for subtle differences on the role of three energetic components (E_{elst} , E_{ind} , and E_{disp}) in tuning the secondary interaction. In summary, the molecular electrostatic potential approach complemented with SAPT decomposition provide a valuable tool to analyse, understand, predict, and modulate secondary interaction.

References

- [1] M. R. Buchner, Recent contributions to the coordination chemistry of beryllium, Chem. – Eur. J. 25 (52) (2019) 12018–12036.
- [2] K. J. Iversen, S. A. Couchman, D. J. Wilson, J. L. Dutton, Modern organometallic and coordination chemistry of beryllium, Coordination Chemistry Reviews 297-298 (2015) 40 – 48.
- [3] I. Alkorta, J. Elguero, M. Yáñez, O. Mó, Cooperativity in beryllium bonds, Phys. Chem. Chem. Phys. 16 (2014) 4305–4312.

- [4] T. Hanusa, E. Bierschenk, L. Engerer, K. Martin, N. Rightmire, 1.37 - alkaline earth chemistry: Synthesis and structures, in: J. Reedijk, K. Poeppelmeier (Eds.), *Comprehensive Inorganic Chemistry II (Second Edition)*, second edition Edition, Elsevier, Amsterdam, 2013, pp. 1133 – 1187.
- [5] M. Yáñez, P. Sanz, O. Mó, I. Alkorta, J. Elguero, Beryllium bonds, do they exist?, *Journal of Chemical Theory and Computation* 5 (10) (2009) 2763–2771.
- [6] A. S. Mahadevi, G. N. Sastry, Cooperativity in noncovalent interactions, *Chemical Reviews* 116 (5) (2016) 2775–2825.
- [7] J. Nochebuena, C. Cuautli, J. Ireta, Origin of cooperativity in hydrogen bonding, *Phys. Chem. Chem. Phys.* 19 (2017) 15256–15263.
- [8] O. Mó, M. Yáñez, I. Alkorta, J. Elguero, Modulating the strength of hydrogen bonds through beryllium bonds, *Journal of Chemical Theory and Computation* 8 (7) (2012) 2293–2300.
- [9] L. Albrecht, R. J. Boyd, O. Mó, M. Yáñez, Cooperativity between hydrogen bonds and beryllium bonds in (h₂o)_nbex₂ (n = 1–3, x = h, f) complexes. a new perspective, *Phys. Chem. Chem. Phys.* 14 (2012) 14540–14547.
- [10] L. Albrecht, R. J. Boyd, O. Mó, M. Yáñez, Changing weak halogen bonds into strong ones through cooperativity with beryllium bonds, *The Journal of Physical Chemistry A* 118 (23) (2014) 4205–4213.
- [11] M. Dressel, S. D. Nogai, R. J. F. Berger, H. Schmidbaur, Beryllium dichloride coordination by nitrogen donor molecules, *Zeitschrift für Naturforschung B* 58 (2003) 173 – 182.
- [12] M. Müller, M. R. Buchner, Solution behavior of beryllium halides in dimethylformamide, *Inorganic Chemistry* 58 (19) (2019) 13276–13284.
- [13] S. A. Couchman, N. Holzmann, G. Frenking, D. J. D. Wilson, J. L. Dutton, Beryllium chemistry the safe way: a theoretical evaluation of low oxidation state beryllium compounds, *Dalton Trans.* 42 (2013) 11375–11384.
- [14] M. Arrowsmith, H. Braunschweig, M. A. Çelik, T. Dellermann, R. D. Dewhurst, W. C. Ewing, K. Hammond, T. Kramer, I. Krummenacher, J. Mies, K. Radacki, J. K. Schuster, Neutral zero-valent s-block complexes with strong multiple bonding., *Nature chemistry* 8 7 (2016) 638–42.
- [15] A. C. Legon, N. R. Walker, What’s in a name? ‘coinage-metal’ non-covalent bonds and their definition, *Phys. Chem. Chem. Phys.* 20 (2018) 19332–19338.
- [16] N. Alcock, *Secondary Bonding to Nonmetallic Elements*, Academic Press, 1972, Ch. 1, pp. 1–58.
- [17] L. Brammer, Halogen bonding, chalcogen bonding, pnictogen bonding, tetrel bonding: origins, current status and discussion, *Faraday Discuss.* 203 (2017) 485–507.
- [18] B. Silvi, E. Alikhani, H. Ratajczak, Towards an unified chemical model of secondary bonding, Submitted to *Journal of Molecular Modeling*.
- [19] M. Müller, M. R. Buchner, Beryllium-induced conversion of aldehydes, *Chemistry – A European Journal* 25 (47) (2019) 11147–11156.

- [20] M. J. Frisch, G. W. Trucks, H. B. Schlegel, G. E. Scuseria, M. A. Robb, J. R. Cheeseman, G. Scalmani, V. Barone, B. Mennucci, G. A. Petersson, H. Nakatsuji, M. Caricato, X. Li, H. P. Hratchian, A. F. Izmaylov, J. Bloino, G. Zheng, J. L. Sonnenberg, M. Hada, M. Ehara, K. Toyota, R. Fukuda, J. Hasegawa, M. Ishida, T. Nakajima, Y. Honda, O. Kitao, H. Nakai, T. Vreven, J. A. Montgomery, Jr., J. E. Peralta, F. Ogliaro, M. Bearpark, J. J. Heyd, E. Brothers, K. N. Kudin, V. N. Staroverov, T. Keith, R. Kobayashi, J. Normand, K. Raghavachari, A. Rendell, J. C. Burant, S. S. Iyengar, J. Tomasi, M. Cossi, N. Rega, J. M. Millam, M. Klene, J. E. Knox, J. B. Cross, V. Bakken, C. Adamo, J. Jaramillo, R. Gomperts, R. E. Stratmann, O. Yazyev, A. J. Austin, R. Cammi, C. Pomelli, J. W. Ochterski, R. L. Martin, K. Morokuma, V. G. Zakrzewski, G. A. Voth, P. Salvador, J. J. Dannenberg, S. Dapprich, A. D. Daniels, O. Farkas, J. B. Foresman, J. V. Ortiz, J. Cioslowski, , D. J. Fox, Gaussian~09 Revision D.01, gaussian Inc. Wallingford CT (2013).
- [21] J. Čížek, On the correlation problem in atomic and molecular systems. calculation of wavefunction components in ursell-type expansion using quantum-field theoretical methods, *The Journal of Chemical Physics* 45 (11) (1966) 4256–4266.
- [22] J. Čížek, On the Use of the Cluster Expansion and the Technique of Diagrams in Calculations of Correlation Effects in Atoms and Molecules, John Wiley & Sons, Ltd, 2007, Ch. 2, pp. 35–89.
- [23] G. D. Purvis, R. J. Bartlett, A full coupled-cluster singles and doubles model: The inclusion of disconnected triples, *The Journal of Chemical Physics* 76 (4) (1982) 1910–1918.
- [24] G. E. Scuseria, C. L. Janssen, H. F. Schaefer, An efficient reformulation of the closed-shell coupled cluster single and double excitation (ccsd) equations, *The Journal of Chemical Physics* 89 (12) (1988) 7382–7387.
- [25] G. E. Scuseria, H. F. Schaefer, Is coupled cluster singles and doubles (ccsd) more computationally intensive than quadratic configuration interaction (qcisd)?, *The Journal of Chemical Physics* 90 (7) (1989) 3700–3703.
- [26] G. D. Purvis, R. J. Bartlett, A full coupled-cluster singles and doubles model: The inclusion of disconnected triples, *The Journal of Chemical Physics* 76 (4) (1982) 1910–1918.
- [27] J. A. Pople, M. Head-Gordon, K. Raghavachari, Quadratic configuration interaction. a general technique for determining electron correlation energies, *The Journal of Chemical Physics* 87 (10) (1987) 5968–5975.
- [28] T. H. Dunning, Gaussian basis sets for use in correlated molecular calculations. i. the atoms boron through neon and hydrogen, *The Journal of Chemical Physics* 90 (2) (1989) 1007–1023.
- [29] A. D. Becke, Density-functional thermochemistry. iii. the role of exact exchange, *The Journal of Chemical Physics* 98 (7) (1993) 5648–5652.
- [30] S. Grimme, S. Ehrlich, L. Goerigk, Effect of the damping function in dispersion corrected density functional theory, *Journal of Computational Chemistry* 32 (7) (2011) 1456–1465.
- [31] F. Weigend, R. Ahlrichs, Balanced basis sets of split valence, triple zeta valence and quadruple zeta valence quality for h to rn: Design and assessment of accuracy, *Phys. Chem. Chem. Phys.* 7 (2005) 3297–3305.

- [32] F. Weigend, Accurate coulomb-fitting basis sets for h to rn, *Phys. Chem. Chem. Phys.* 8 (2006) 1057–1065.
- [33] J. M. Turney, A. C. Simmonett, R. M. Parrish, E. G. Hohenstein, F. A. Evangelista, J. T. Fermann, B. J. Mintz, L. A. Burns, J. J. Wilke, M. L. Abrams, N. J. Russ, M. L. Leininger, C. L. Janssen, E. T. Seidl, W. D. Allen, H. F. Schaefer, R. A. King, E. F. Valeev, C. D. Sherrill, T. D. Crawford, Psi4: an open-source ab initio electronic structure program, *Wiley Interdisciplinary Reviews: Computational Molecular Science* 2 (4) (2012) 556–565.
- [34] T. M. Parker, L. A. Burns, R. M. Parrish, A. G. Ryno, C. D. Sherrill, Levels of symmetry adapted perturbation theory (sapt). i. efficiency and performance for interaction energies, *The Journal of Chemical Physics* 140 (9) (2014) 094106.
- [35] J. M. Turney, A. C. Simmonett, R. M. Parrish, E. G. Hohenstein, F. A. Evangelista, J. T. Fermann, B. J. Mintz, L. A. Burns, J. J. Wilke, M. L. Abrams, N. J. Russ, M. L. Leininger, C. L. Janssen, E. T. Seidl, W. D. Allen, H. F. Schaefer, R. A. King, E. F. Valeev, C. D. Sherrill, T. D. Crawford, Psi4: an open-source ab initio electronic structure program, *Wiley Interdisciplinary Reviews: Computational Molecular Science* 2 (4) (2012) 556–565.
- [36] R. M. Parrish, L. A. Burns, D. G. A. Smith, A. C. Simmonett, A. E. DePrince, E. G. Hohenstein, U. Bozkaya, A. Y. Sokolov, R. Di Remigio, R. M. Richard, J. F. Gonthier, A. M. James, H. R. McAlexander, A. Kumar, M. Saitow, X. Wang, B. P. Pritchard, P. Verma, H. F. Schaefer, K. Patkowski, R. A. King, E. F. Valeev, F. A. Evangelista, J. M. Turney, T. D. Crawford, C. D. Sherrill, Psi4 1.1: An open-source electronic structure program emphasizing automation, advanced libraries, and interoperability, *Journal of Chemical Theory and Computation* 13 (7) (2017) 3185–3197.
- [37] T. A. Keith, Imall (version 19.10.12), todd a. keith, tk gristmill software, overland park ks, usa, 2019 (aim.tkgristmill.com).
- [38] T. Lu, F. Chen, Multiwfn: A multifunctional wavefunction analyzer, *Journal of Computational Chemistry* 33 (5) (2012) 580–592.
- [39] R. F. W. Bader, *Atoms in Molecules: a Quantum Theory*, CLARENDON PRESS, Oxford University Press Inc., New York, United States, 1994.
- [40] R. F. W. Bader, Definition of molecular structure: By choice or by appeal to observation?, *The Journal of Physical Chemistry A* 114 (28) (2010) 7431–7444.
- [41] A. D. Becke, K. E. Edgecombe, A simple measure of electron localization in atomic and molecular systems, *The Journal of Chemical Physics* 92 (9) (1990) 5397–5403.
- [42] S. Noury, X. Krokidis, F. Fuster, B. Silvi, Computational tools for the electron localization function topological analysis, *Computers & Chemistry* 23 (6) (1999) 597 – 604.
- [43] B. Silvi, A. Savin, Classification of chemical bonds based on topological analysis of electron localization functions, *The Journal of Chemical Physics* 371 (-) (1994) 683–686.
- [44] E. Alikhani, F. Fuster, B. Madebene, S. J. Grabowski, Topological reaction sites – very strong chalcogen bonds, *Phys. Chem. Chem. Phys.* 16 (2014) 2430–2442.
- [45] A. Bauzá, A. Frontera, Aerogen bonding interaction: A new supramolecular force?, *Angewandte Chemie International Edition* 54 (25) (2015) 7340–7343.

- [46] A. Bauzá, A. Frontera, π -hole aerogen bonding interactions, *Phys. Chem. Chem. Phys.* 17 (2015) 24748–24753.
- [47] R. Saha, G. Jana, S. Pan, G. Merino, P. K. Chattaraj, How far can one push the noble gases towards bonding?: A personal account, *Molecules* 24 (16) (2019) 2933.
- [48] P. Antoniotti, N. Bronzolino, F. Grandinetti, Stable compounds of the lightest noble gases: A computational investigation of rnbeng (ng = he, ne, ar), *The Journal of Physical Chemistry A* 107 (16) (2003) 2974–2980.
- [49] M. H. Jamróz, *Vibrational Energy Distribution Analysis VEDA 4*, 2004.
- [50] M. H. Jamróz, *Vibrational energy distribution analysis (VEDA): scopes and limitations*, *Spectrochimica Acta Part A: Molecular and Biomolecular Spectroscopy* 114 (10) (2013) 220–230.
- [51] G. Frenking, W. Koch, J. Gauss, D. Cremer, Stabilities and nature of the attractive interactions in hebeo, nebeo, and arbeo and a comparison with analogs nglif, ngbn, and nglih (ng = he, ar). a theoretical investigation, *Journal of the American Chemical Society* 110 (24) (1988) 8007–8016.
- [52] R. F. W. Bader, Atoms in molecules, *Accounts of Chemical Research* 18 (1) (1985) 9–15.
- [53] S. Borocci, N. Bronzolino, F. Grandinetti, From obehe to h3bobehe: Enhancing the stability of a neutral helium compound, *Chemical Physics Letters* 406 (1) (2005) 179 – 183.
- [54] T. Clark, J. S. Murray, P. Politzer, A perspective on quantum mechanics and chemical concepts in describing noncovalent interactions, *Phys. Chem. Chem. Phys.* 20 (2018) 30076–30082.
- [55] P. Politzer, J. S. Murray, T. Clark, G. Resnati, The σ -hole revisited, *Phys. Chem. Chem. Phys.* 19 (2017) 32166–32178.
- [56] M. Müller, M. R. Buchner, Preparation and crystal structures of the beryllium amines [be(nh3)4]x2 (x = br, i, cn, scn, n3) and be(nh3)2x'2 (x' = cl, br, i), *Chem. Commun.* (2019) –.
- [57] S. Grabowski, An estimation of strength of intramolecular hydrogen bonds — ab initio and aim studies, *Journal of Molecular Structure* 562 (1) (2001) 137 – 143.
- [58] S. J. Grabowski, Qtaim characteristics of halogen bond and related interactions, *The Journal of Physical Chemistry A* 116 (7) (2012) 1838–1845.
- [59] F. Fuster, S. J. Grabowski, Intramolecular hydrogen bonds: the qtaim and elf characteristics, *The Journal of Physical Chemistry A* 115 (35) (2011) 10078–10086.
- [60] M. Yáñez, O. Mó, I. Alkorta, J. Elguero, Can conventional bases and unsaturated hydrocarbons be converted into gas-phase superacids that are stronger than most of the known oxyacids? the role of beryllium bonds, *Chemistry – A European Journal* 19 (35) (2013) 11637–11643.
- [61] I. Alkorta, J. Elguero, O. Mó, M. Yáñez, J. E. Del Bene, Using beryllium bonds to change halogen bonds from traditional to chlorine-shared to ion-pair bonds, *Phys. Chem. Chem. Phys.* 17 (2015) 2259–2267.

- [62] K. Eskandari, Nature of beryllium bonds in view of interacting quantum atoms and natural energy decomposition analysis, *Computational and Theoretical Chemistry* 1090 (2016) 74–79.
- [63] A. M. Lamsabhi, M. M. Vallejos, B. Herrera, O. M3, M. Y3ñez, Effect of beryllium bonds on the keto–enol tautomerism of formamide derivatives: a subtle basicity–acidity balance, *Theoretical Chemistry Accounts* 135 (6) (2016) 147.
- [64] M. Mar3n-Luna, I. Alkorta, J. Elguero, Cooperativity in tetrel bonds, *The Journal of Physical Chemistry A* 120 (4) (2016) 648–656.
- [65] M. M. Montero-Campillo, O. Brea, O. M3, I. Alkorta, J. Elguero, M. Y3ñez, Modulating the intrinsic reactivity of molecules through non-covalent interactions, *Phys. Chem. Chem. Phys.* 21 (2019) 2222–2233.
- [66] I. Alkorta, J. Elguero, M. Solimannejad, Dihydrogen bond cooperativity in (hccbeh)_n clusters, *The Journal of Chemical Physics* 129 (6) (2008) 064115.
- [67] I. Alkorta, F. Blanco, J. Elguero, Dihydrogen bond cooperativity in aza-borane derivatives, *The Journal of Physical Chemistry A* 114 (32) (2010) 8457–8462.